International Conference 2025
Technologies for the Sustainable Use of Natural Resources

International Conference 2025

Development of High-Efficiency Graphene-Based Photothermal Composites for Sustainable Solar Desalination Technologies

Q.T. Tran

Postgraduate student, junior researcher at the National Research University “Moscow Power Engineering Institute”

Moscow, 2025

Relevance of the study

The shortage of fresh water remains one of the most pressing global issues of the 21st century, especially in regions where there is no developed water supply and energy infrastructure. This necessitates the creation of energy-efficient, environmentally friendly, and technologically simple systems for obtaining fresh water. One of the most promising areas in this context is solar desalination, which uses renewable solar energy and minimizes the impact on natural resources.

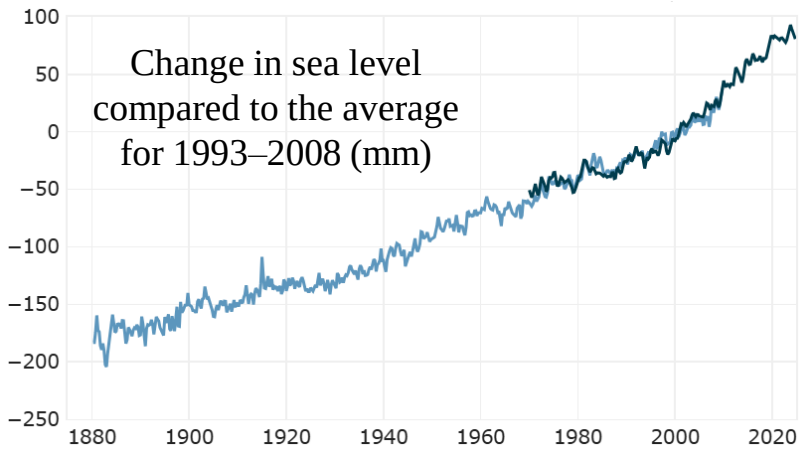

By 2050, more than five billion people on Earth will experience water shortages to some degree
(Source: World Meteorological Organization)

Research objectives and tasks

The main objective is to develop and test graphene composites and study the process of heat and mass transfer during interphase solar vaporization, with a focus on seawater desalination.

Tasks set:

1. Develop materials for interphase solar evaporators based on graphene composites with two- and three-dimensional capillary channel architecture, investigate their capillary and transport characteristics.

2. Conduct experimental studies of heat and mass transfer in the developed solar evaporators, evaluate their performance when working with distilled and salt water, the efficiency of photothermal conversion, and resistance to salt deposition.

3. Develop and verify heat and mass transfer models in the interphase solar evaporation zone, conduct a parametric analysis of the influence of design, thermophysical, and external factors on the intensity of vaporization.

Interphase solar water vapor generation

Solar distillation is a promising technology for obtaining fresh water in conditions of resource scarcity. Nanostructured materials increase its efficiency by enhancing radiation absorption and reducing heat loss.

Basic requirements for solar evaporators:

1. Maximum solar radiation absorption.
2. Minimal heat loss.
3. Durability and resistance to salt deposits and external influences.
4. Cost-effectiveness and technological accessibility.

→ **Maximum photothermal conversion efficiency**

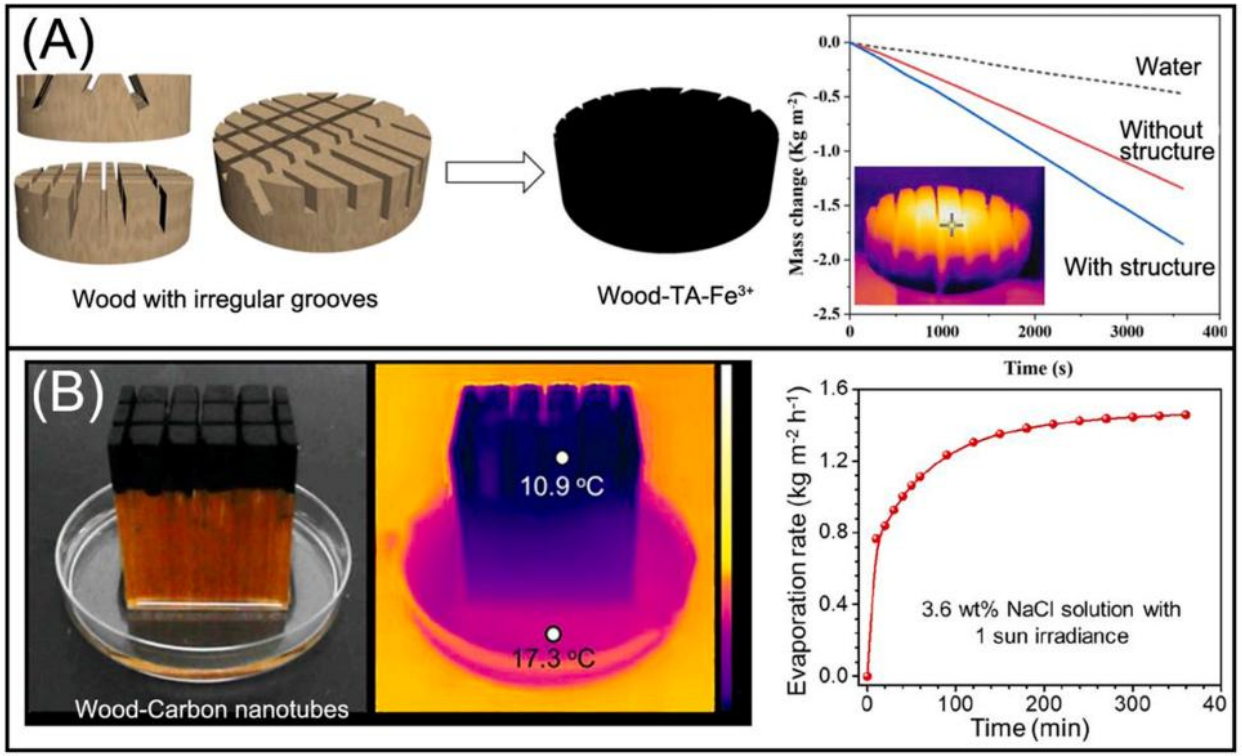

Modified wood surface with photothermal layers: (A) composition based on tannic acid and iron (II) sulfate, (B) layer of carbon nanotubes [1]

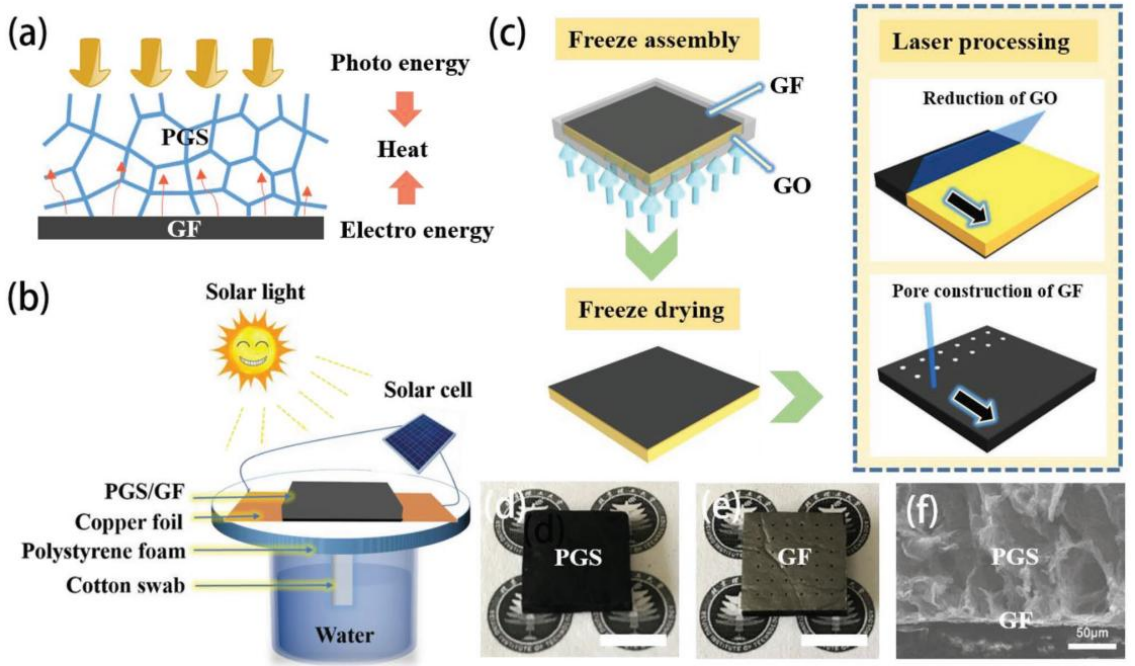

a) Schematic diagram of the photoelectrothermal effect on a hybrid PGS/GF graphene architecture. b) Schematic diagram of a photoelectrothermal solar steam generation system. c) PGS/GF manufacturing process. d, e) Images of the PGS and GF surfaces of the PGS/GF sample, respectively. Scale bar: 1 cm. f) Scanning electron microscopy (SEM) image of a side view of PGS/GF [2].

1. Dong, Y., Tan, Y., Wang, K., Cai, Y., Li, J., Sonne, C., Li, C. (2022). Reviewing wood-based solar-driven interfacial evaporators for desalination. Water Research, 223, 119011.
2. Cui, L., Zhang, P., Xiao, Y., Liang, Y., Liang, H., Cheng, Z., Qu, L. (2018). High rate production of clean water based on the combined photo-electro-thermal effect of graphene architecture. Advanced materials, 30(22), 1706805.

Comparison of 2D and 3D evaporator characteristics

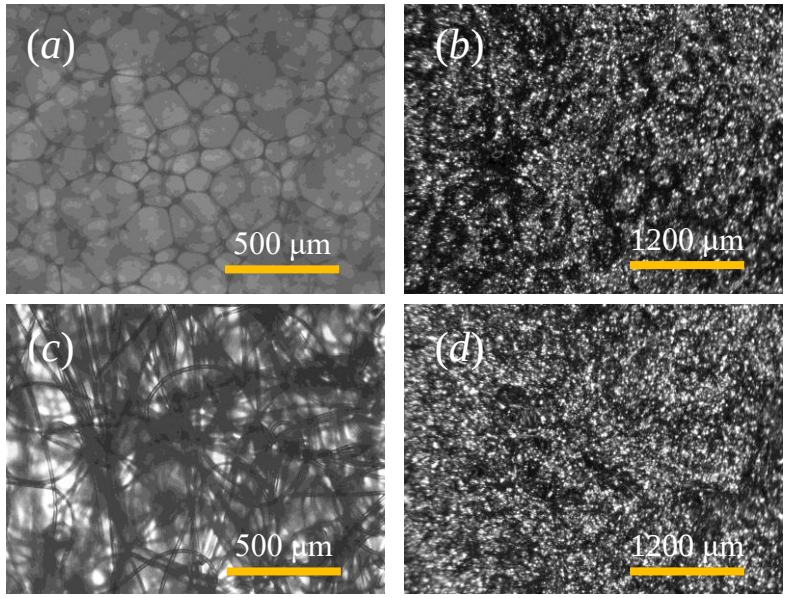

Fig. 1. Samples of evaporators (b, d) based on 3D (melamine sponge - a) and 2D (cotton-based nonwoven material - c) water channels

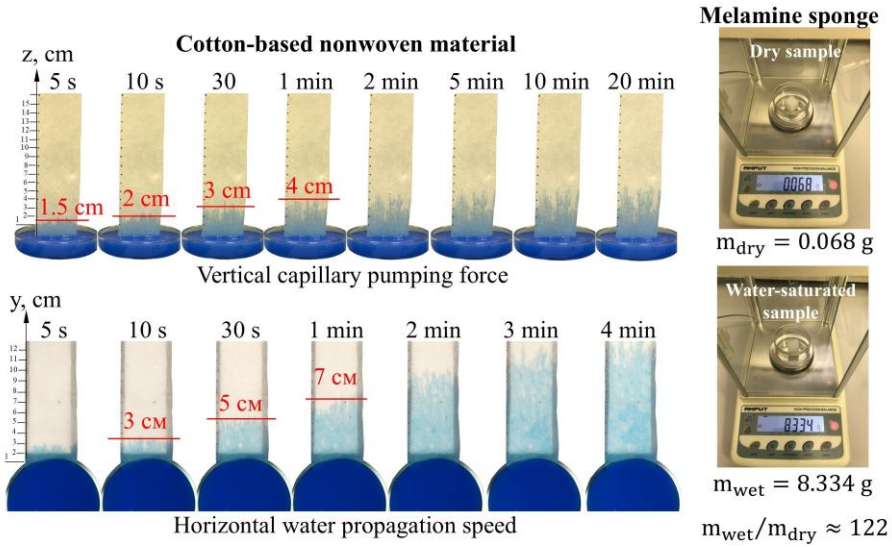

Fig. 2. Assessment of water wettability of materials for solar evaporators

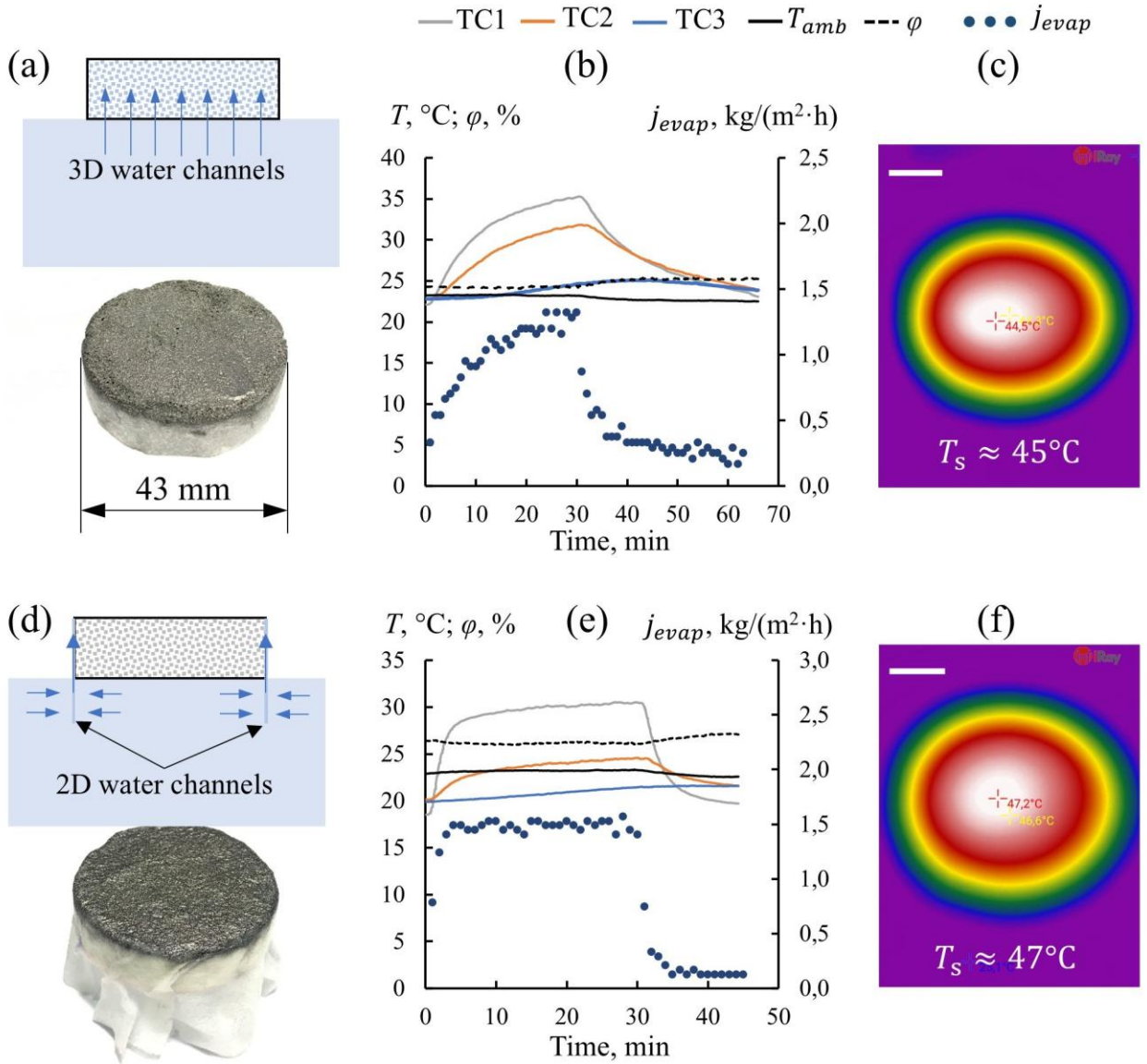

Fig. 3. Comparison of the performance of solar evaporators based on three-dimensional (a – melamine sponge with graphene flakes localized near the surface, b – dynamics of evaporator temperature and evaporation rate, c – evaporator surface temperature) and two-dimensional (d, e, f) water channels: scale bar – 1 cm

Characteristics of interphase solar vaporization on distilled water

Standard solar radiation flux 1000 W/m²

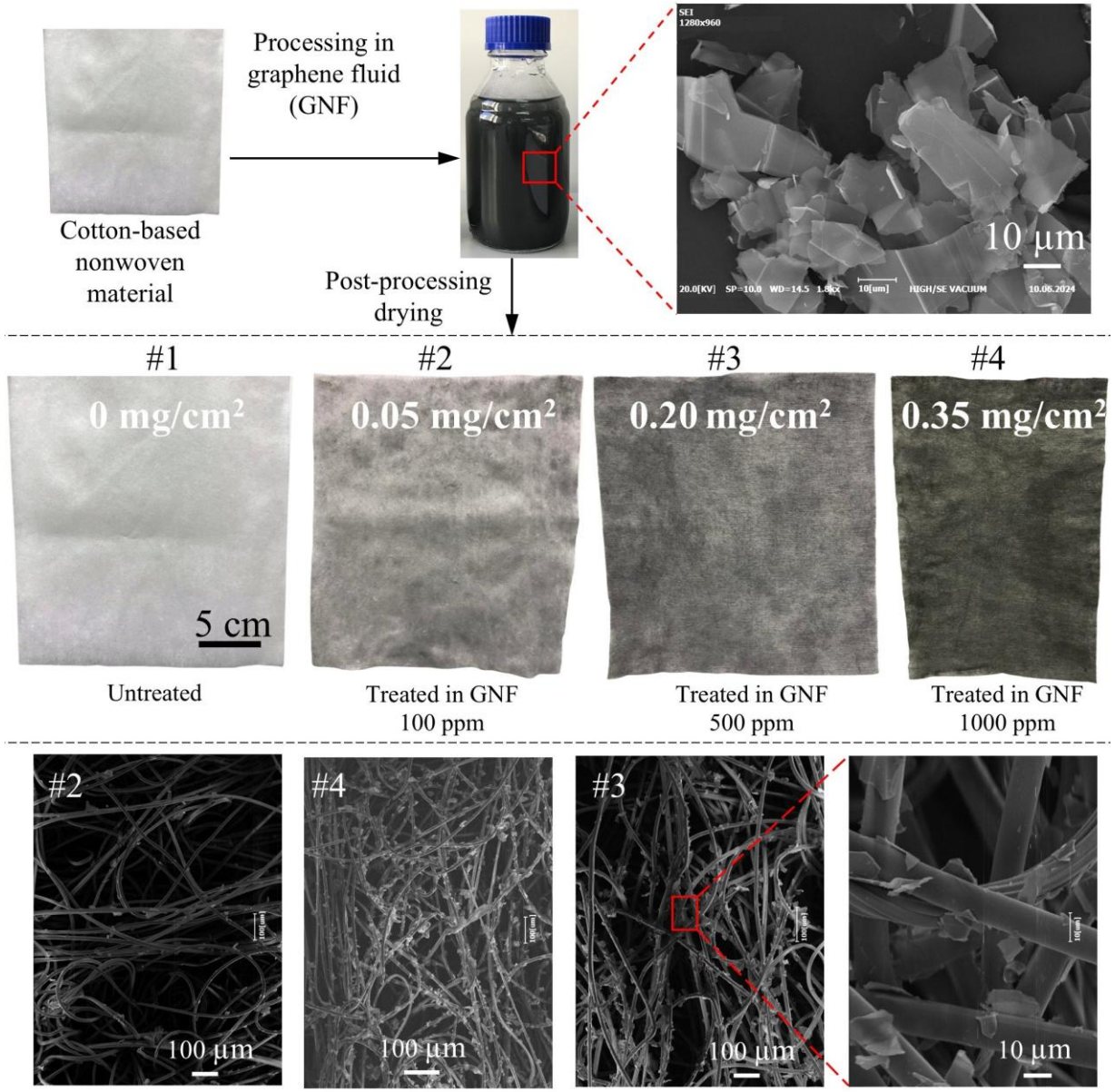

Fig. 1. Nonwoven material processing, appearance, and SEM images of samples for creating a 2D solar evaporator

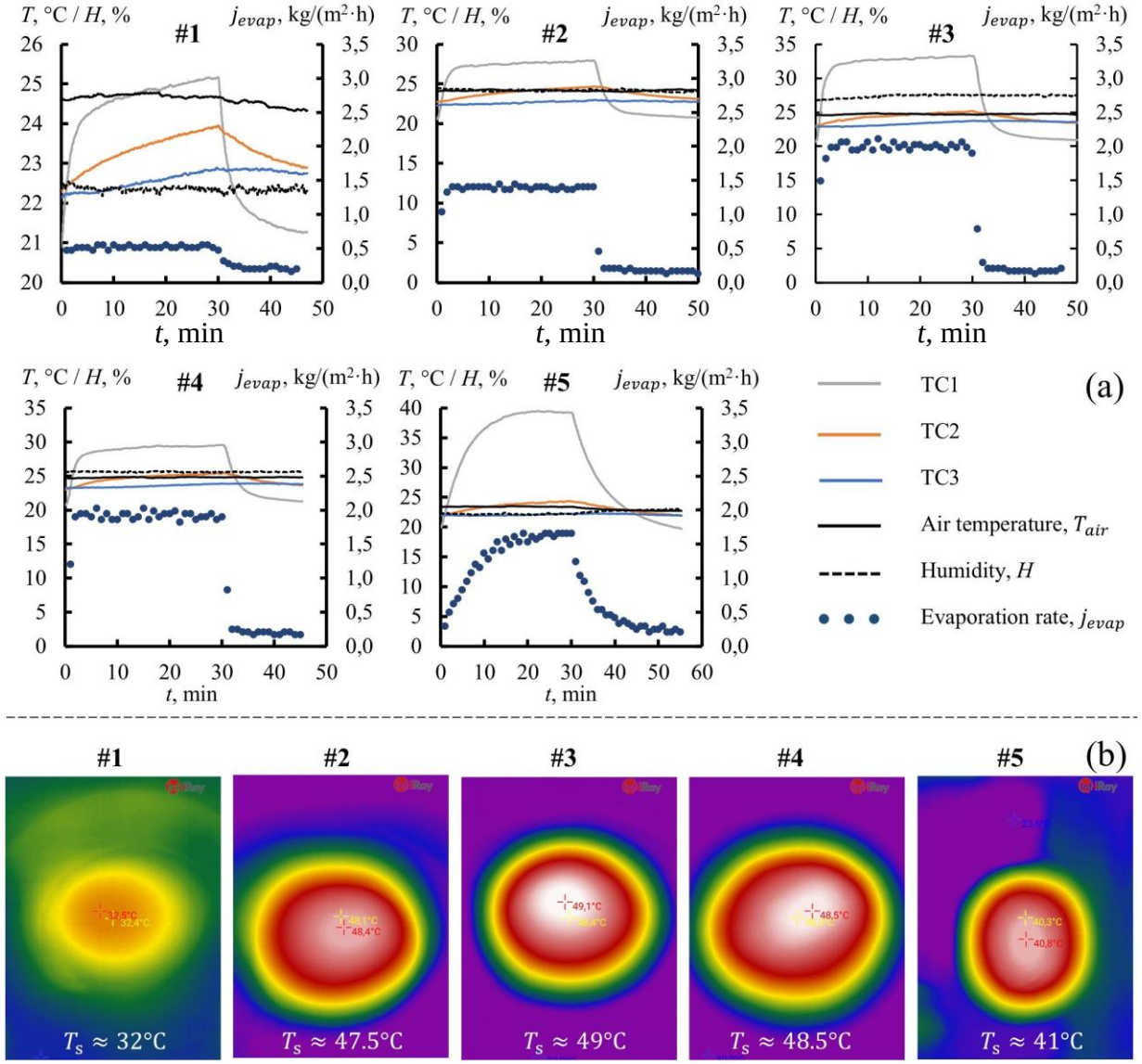

Fig. 2. Heating and evaporation kinetics in two-dimensional solar evaporators at a radiation density of 1000 W/m² (sample #5: 5 mm layer of graphene paste). Scale – 1 cm.

Calculation of photothermal conversion efficiency and solar energy losses

Photothermal efficiency of the vaporization process:

$$\eta_t = \frac{(j_m - j'_m) \cdot h_{eff}}{q_{solar}}, \quad (1)$$

where j_m, j'_m – evaporation rate under solar radiation with density q_{solar} and without radiation, respectively; h_{eff} – actual enthalpy of evaporation of water in the evaporator structure.

- heat loss ratio: $\gamma_{t.l} = \frac{q_{loss}}{q_{solar}}, \quad (2)$

$$q_{loss} = \lambda_l \frac{\Delta T}{\Delta z}, \quad (3)$$

- optical loss ratio: $\gamma_{o.l} = 1 - \eta_t - \gamma_{t.l}. \quad (4)$

Estimation of vaporization enthalpy of water in the evaporator structure:

$$L(T) = \int_{T}^{373.15K} c_{p,l}(T)dT + L(373.15K) + \int_{373.15K}^{T} c_{p,v}(T)dT \quad (5)$$

$$\frac{L_{eff} \cdot m_{sample}}{S_{sample}} = \frac{L(T) \cdot m_{water}}{S_{water}} \quad (6)$$

$$h_{eff} = L_{eff} + h_{sh}. \quad (7)$$

where $L(T), L_{eff}$ – latent heat of vaporization for bulk water and water in the evaporator material matrix, respectively; m_{sample} and m_{water} – mass loss of the evaporator sample and bulk water, respectively, and S_{sample} and S_{water} denote the corresponding evaporation surface areas; h_{sh} – specific heat of heating the liquid from the initial temperature to the evaporation surface temperature.

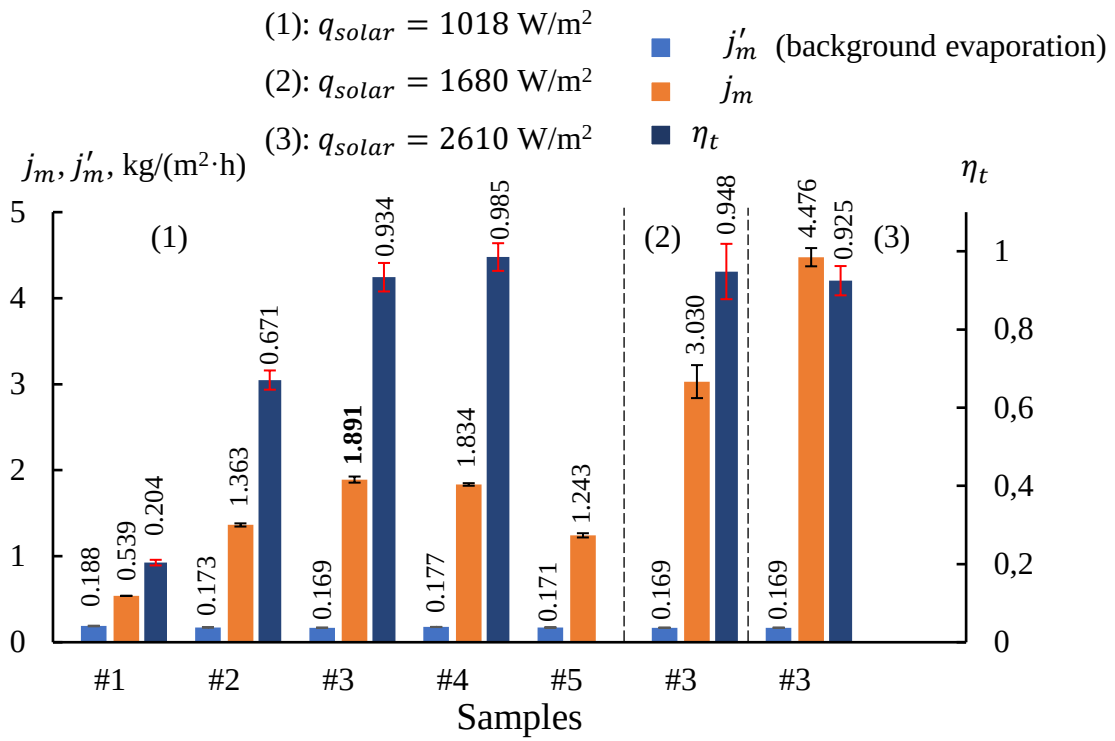

Table 1. Calculation of solar energy losses

q_{solar}, W/m²	Sample	$\gamma_{t.l}$	$\gamma_{o.l}$
1018	#1	0.024	0.772
1018	#2	0.038	0.291
1018	#3	0.035	0.031
1018	#4	0.034	-0.019*
1680	#3	0.035	0.017
2610	#3	0.023	0.052

* Negative values of optical losses are due to errors in the calculation of η associated with the uncertainty of the effective enthalpy of evaporation.

Efficiency and operational stability of a 2D evaporator in saline solutions

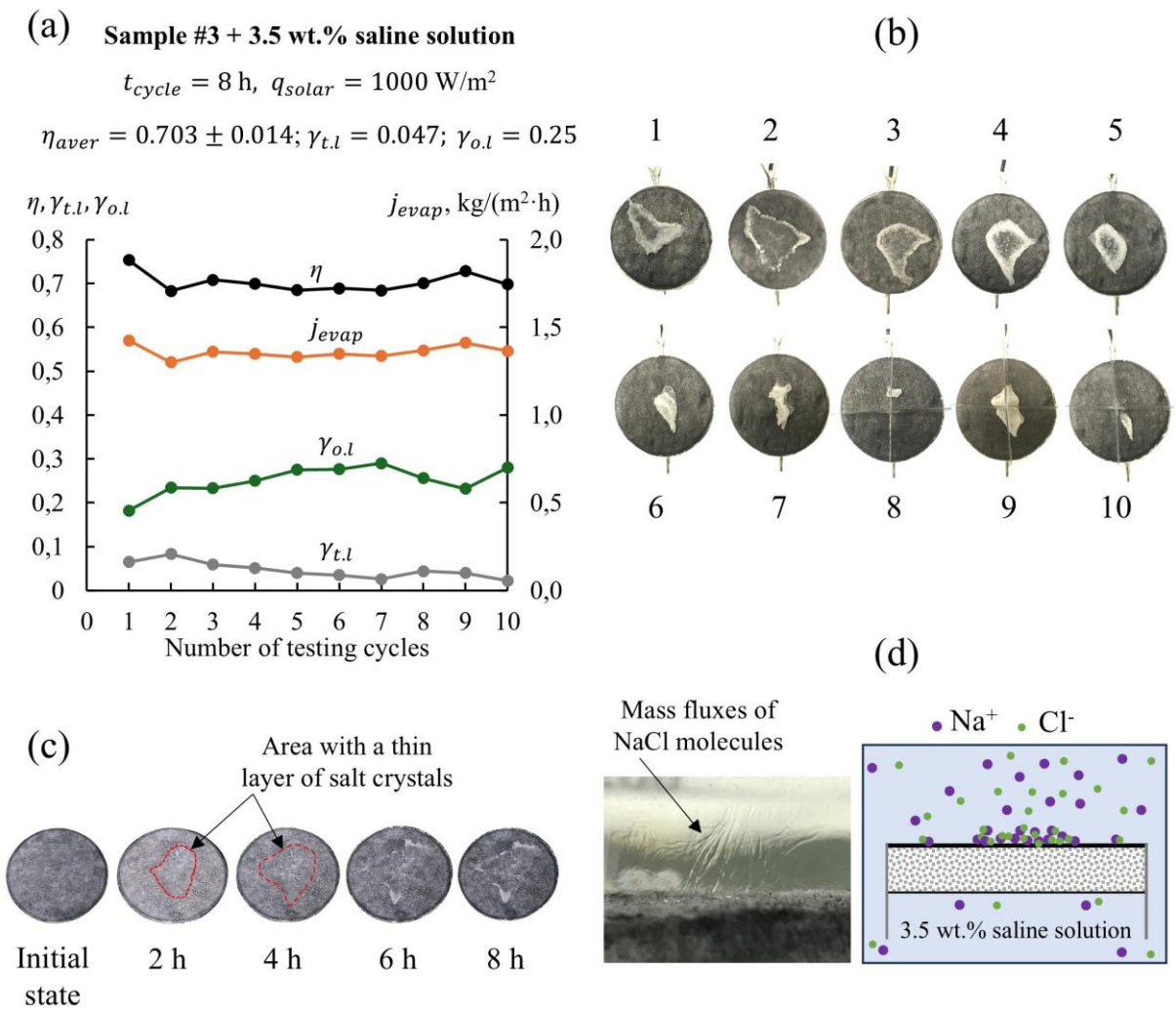

Fig. 1. Results of the evaluation of the 2D evaporator based on material #3 when working with a 3.5% salt solution (a). Final state of the evaporator after each cycle (b) and dynamics of salt formation in the second test cycle (c). Process of salt removal after each cycle by reverse diffusion into the original salt solution (d).

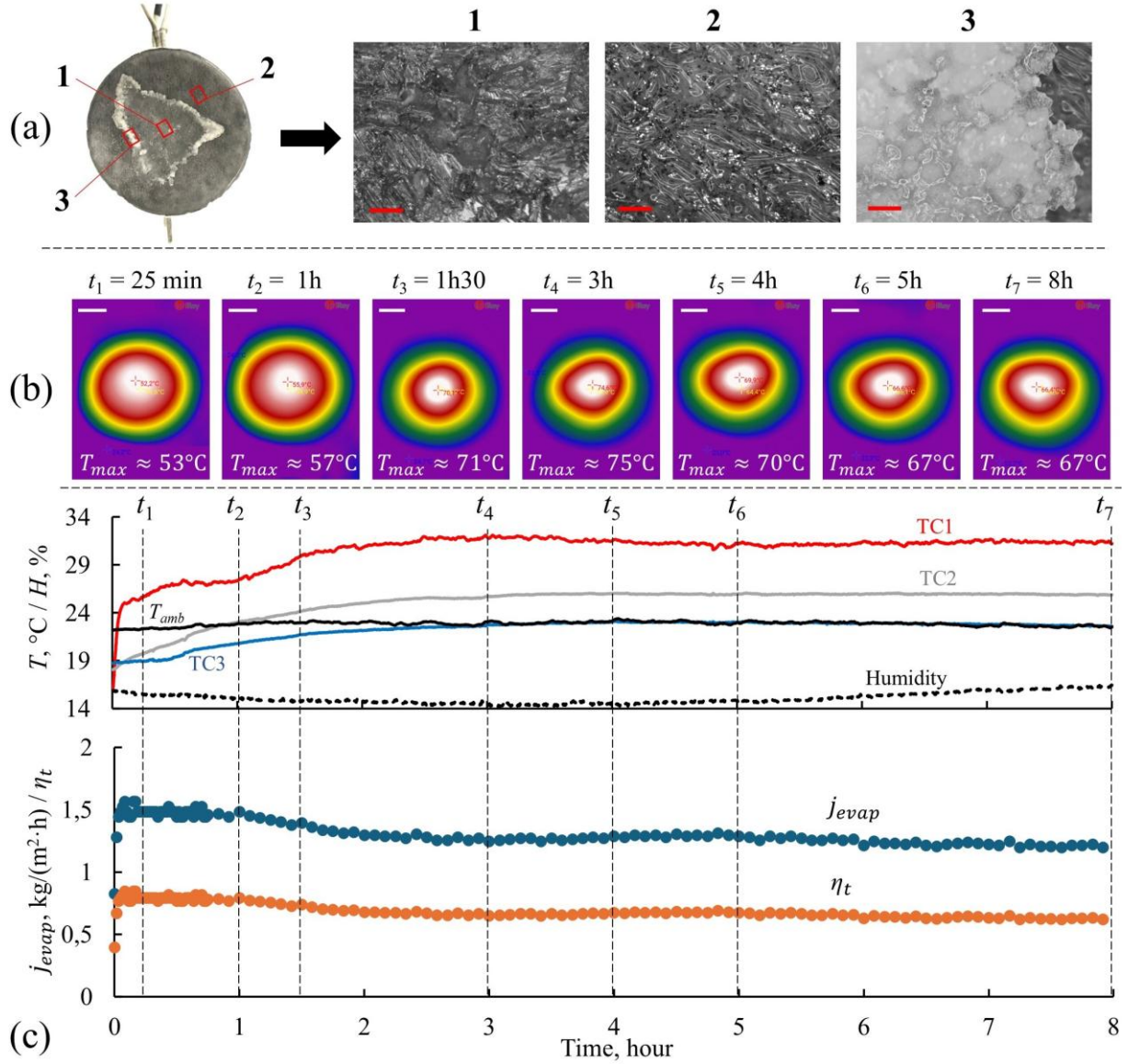

Fig. 2. Morphology of salt crystals (a); temperature profiles (b); evaporation rate and conversion efficiency in the second cycle (c).

Evaporation from the surface of composite hydrogels

Table. Sample characteristics

Sample	Composition	Mass ratio of components
#C1	PVA:PEG:DW	1:1:4
#C2	PVA:PEG:DW: diamond nanoparticles	1:1:4:0,1
#C3	PVA:PEG:DW: graphene flakes	1:1:4:0,1

PVA – polyvinyl alcohol; **PEG** – polyethylene glycol; **DW** – distilled water

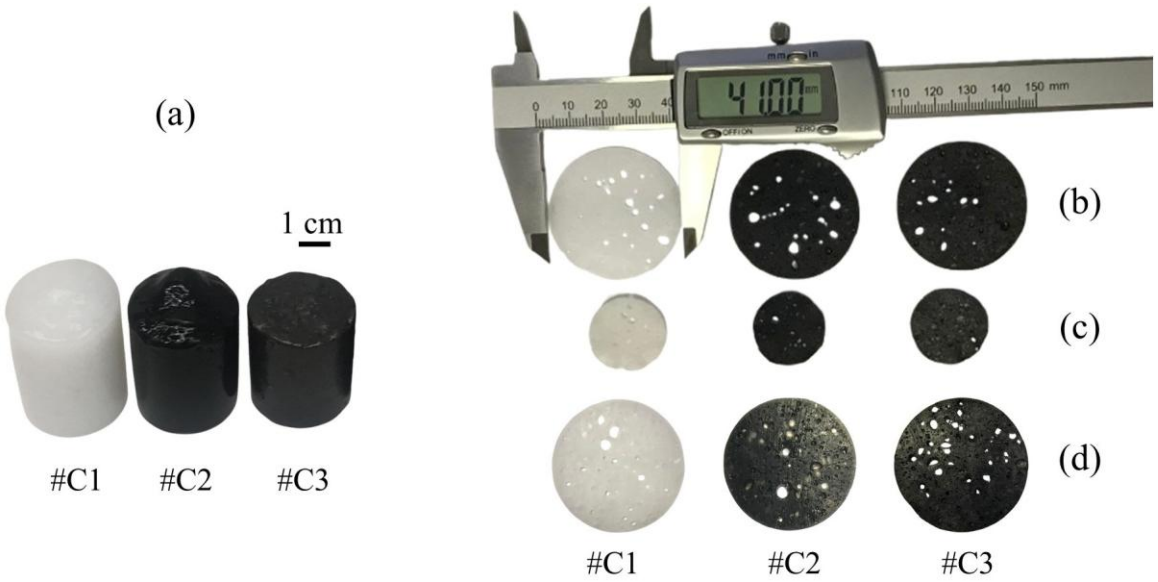

Fig. 1. Overall view of the obtained volumetric samples (a) and their cross-sections: in their initial state (b), after complete drying (c), and after re-saturation with water (d).

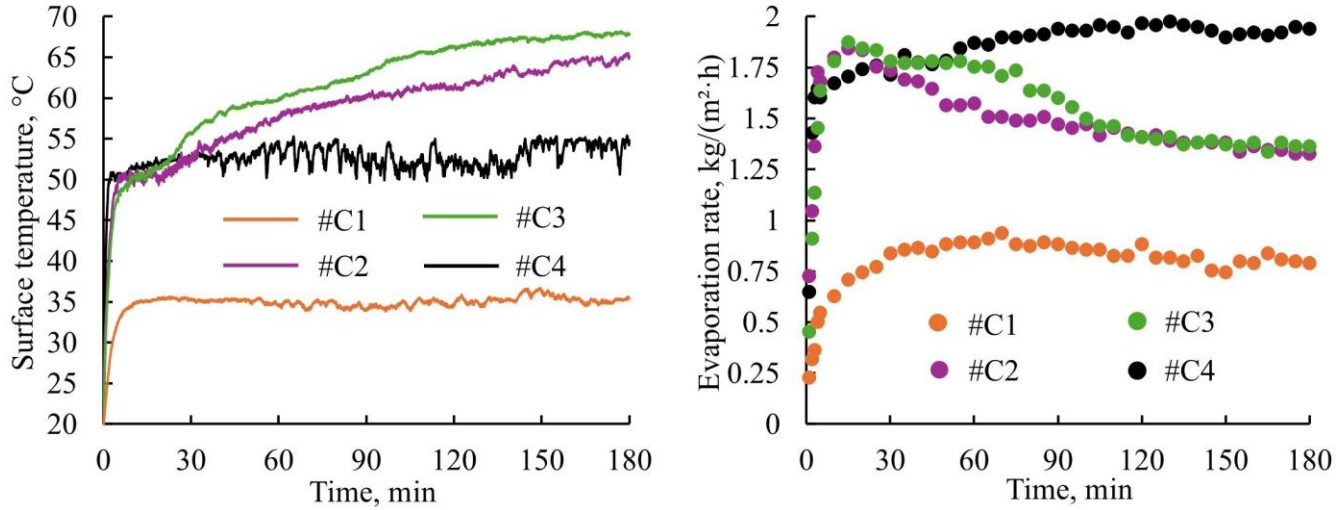

Fig. 2. Dynamics of surface temperature and evaporation rate for samples #C1–C4. (Sample C4 is a nonwoven material modified with graphene flakes with a density of 0.2 mg/m^2.)

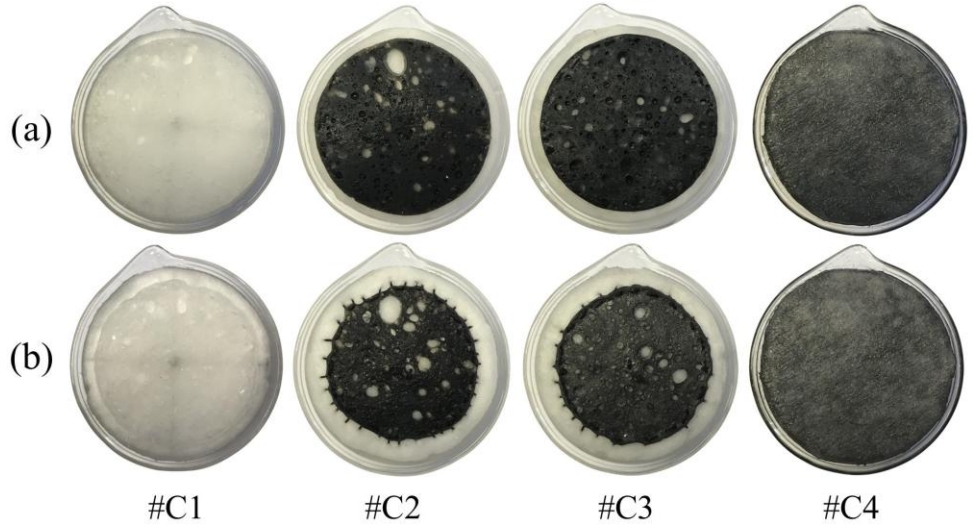

Fig. 3. Comparative morphology of the surface of samples: initial state (a) and after 3 hours of irradiation (b).

Graphene hydrogel membranes for improving the efficiency and stability of solar evaporation

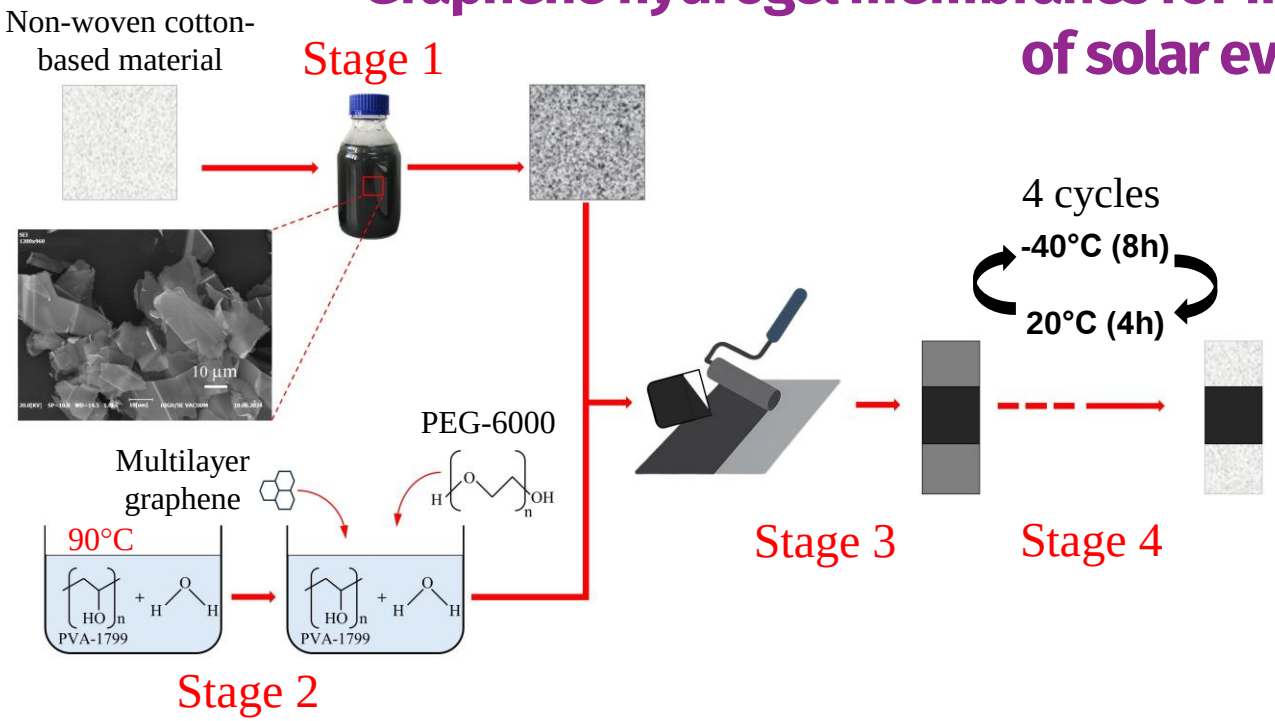

Fig. 1. Stages of graphene-hydrogel membrane formation

Table. Sample characteristics

Sample	Composition	Mass ratio of components
#1	PVA:PEG:DW: graphene flakes	8:8:32:0.1
#2		8:8:32:0.25
#3		8:8:32:0.5

PVA – polyvinyl alcohol; **PEG** – polyethylene glycol; **DW** – distilled water.

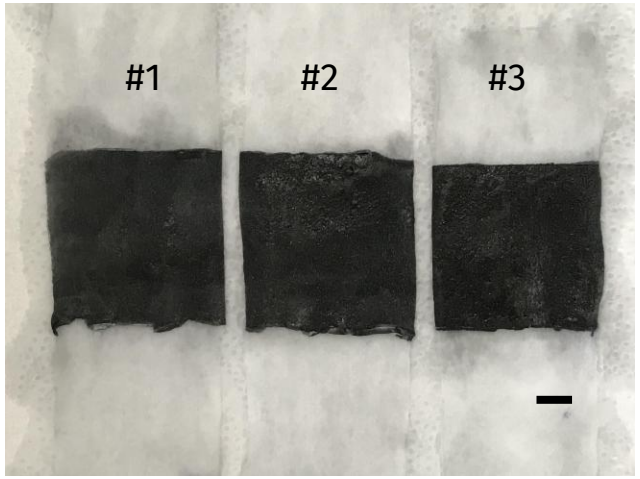

Fig. 2. Samples of graphene-hydrogel composite membranes after cleaning, scale: 1 cm.

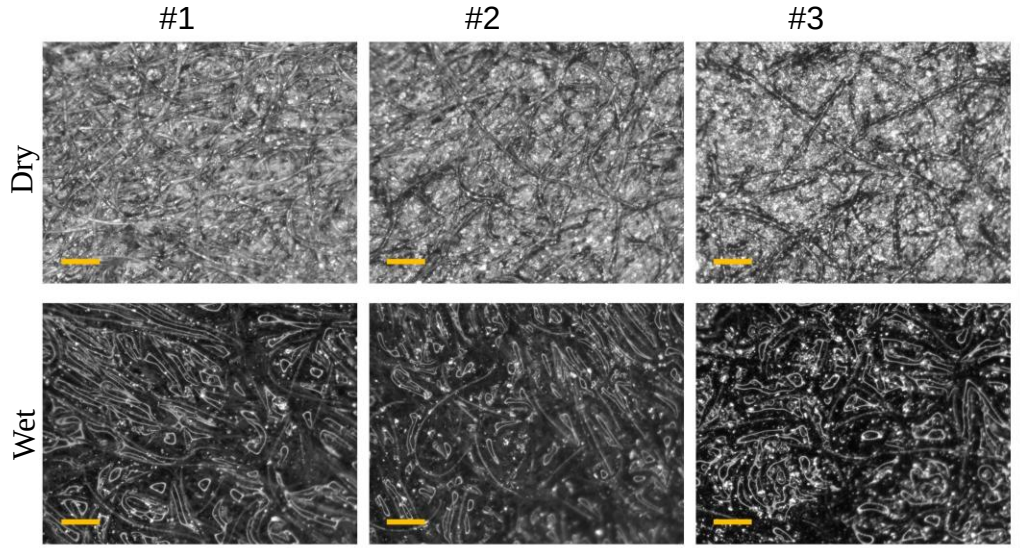

Fig. 3. Surface morphology of samples (scale: 200 µm).

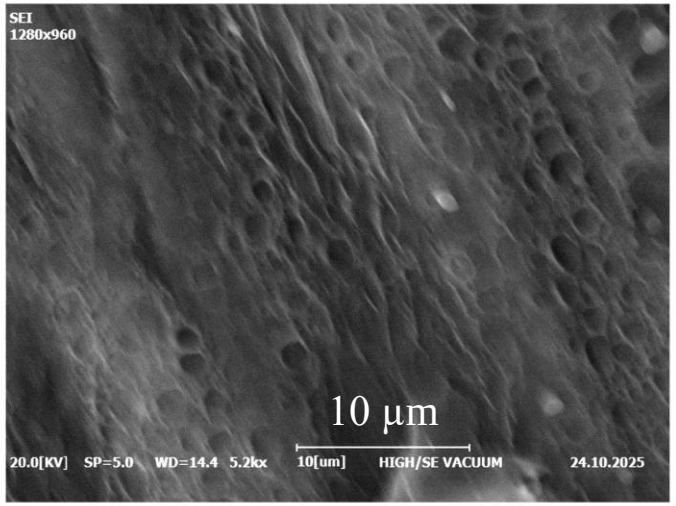

Fig. 3. Micropores in the structure of PVA-PEG hydrogel

Graphene hydrogel membranes for improving the efficiency and stability of solar evaporation

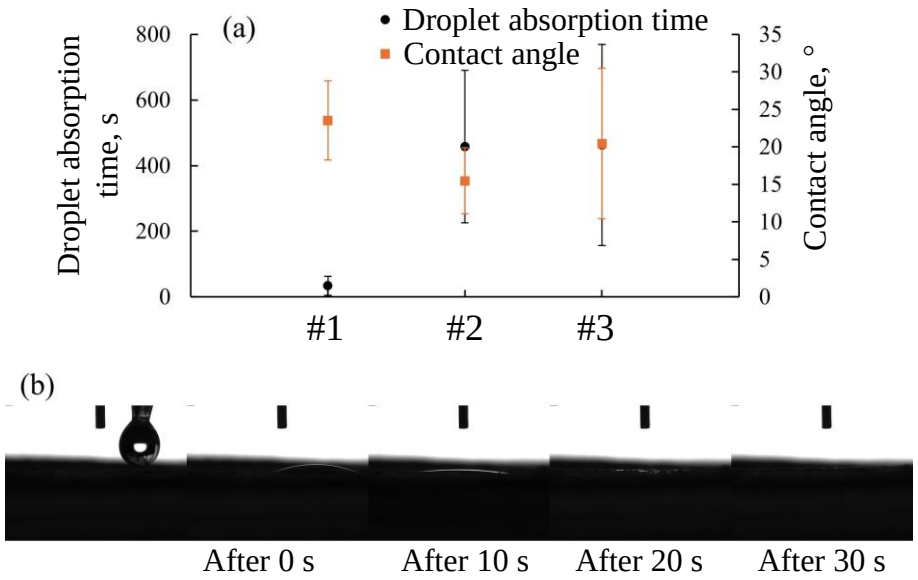

Fig. 1. Wettability and water absorption by membranes (a). The process of absorption of a 5 μl water droplet on the surface of membrane #1 (b).

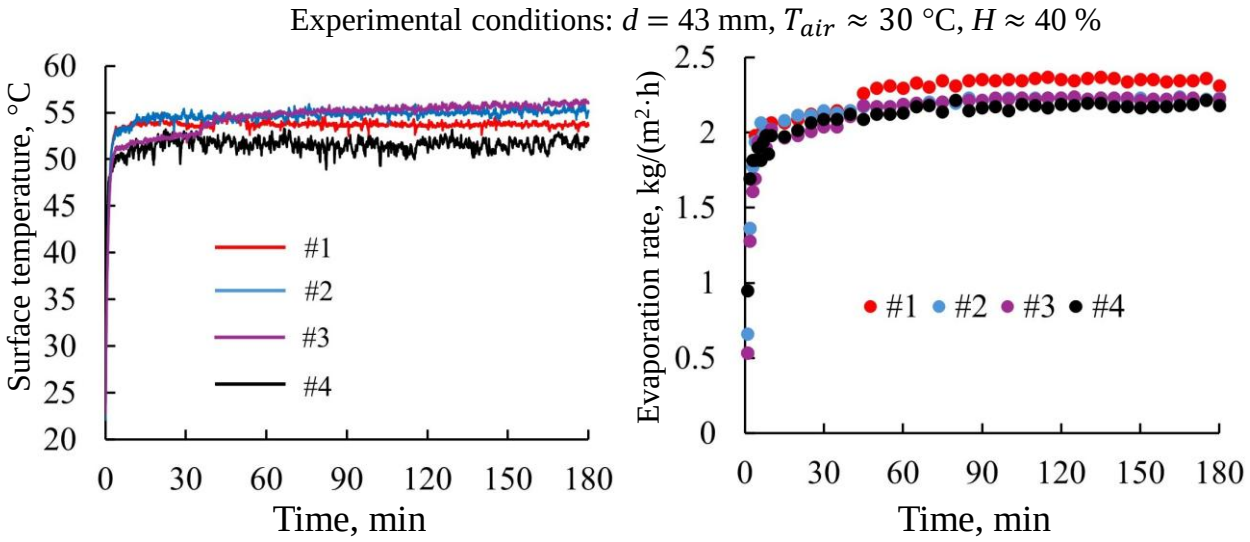

Fig. 2. Operating characteristics of membranes with distilled water.

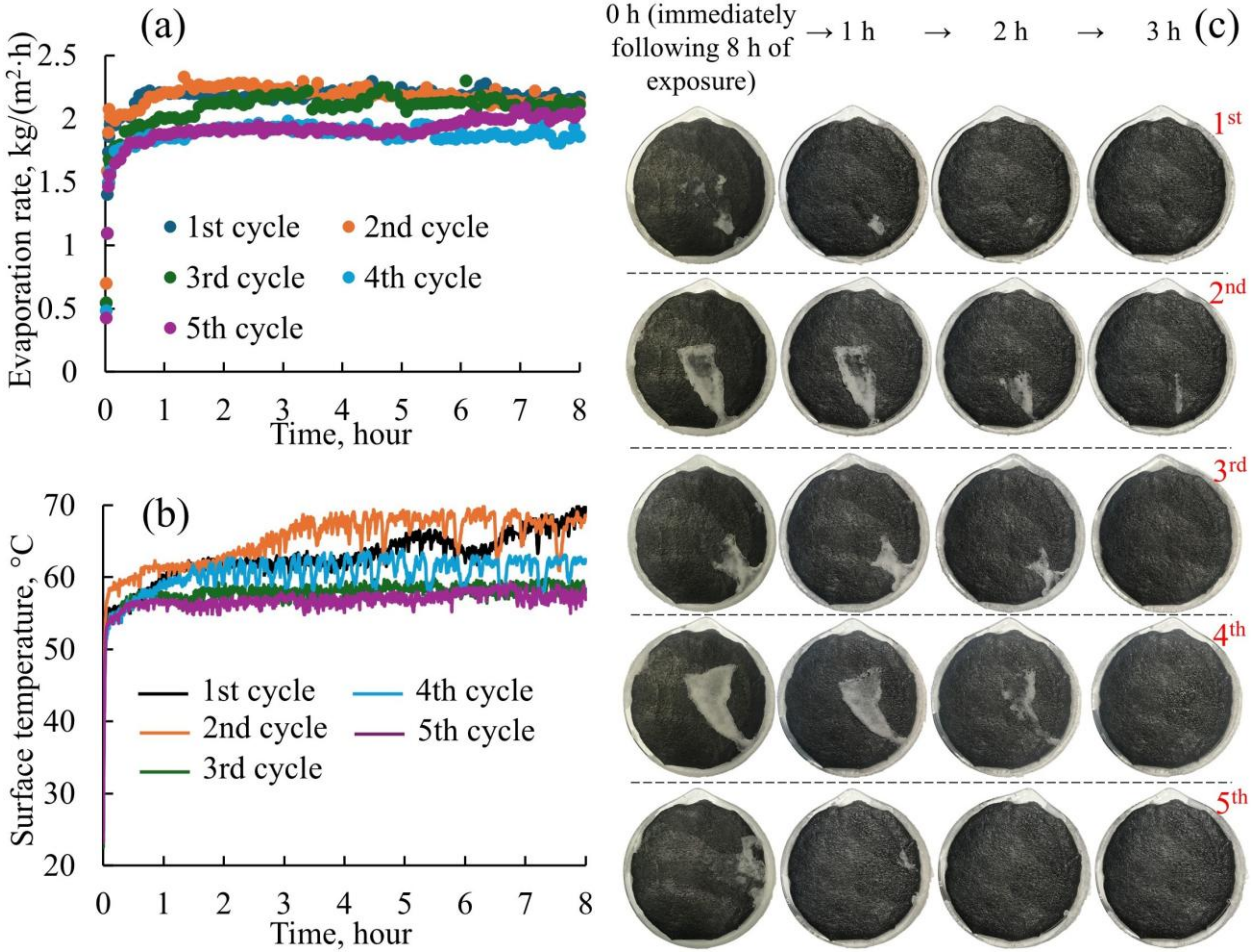

Fig. 3. Test results for membrane #1 during evaporation of a 3.5% NaCl solution

Graphene hydrogel membranes for improving the efficiency and stability of solar evaporation

Evaporation zone optimization

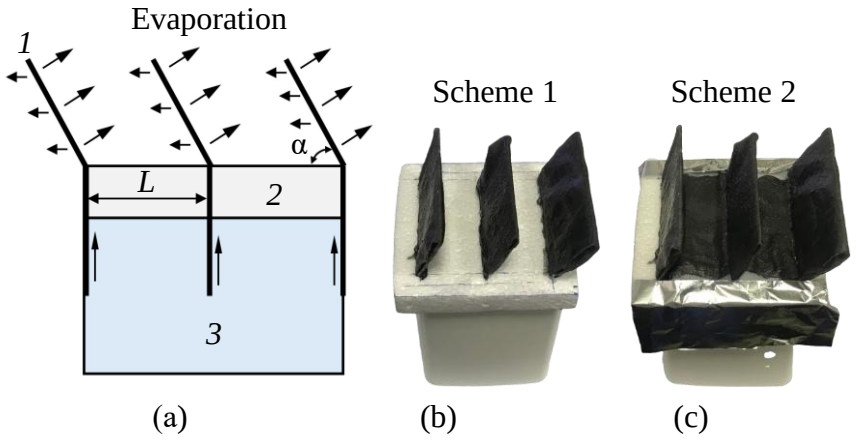

Fig. 1. Configuration of the experimental evaporation zone:
a) layout of elements: 1 – graphene-hydrogel membrane; 2 – floating heat insulation platform; 3 – feed liquid;
b) basic configuration without horizontal membranes;
c) configuration with additional horizontal evaporation zones.

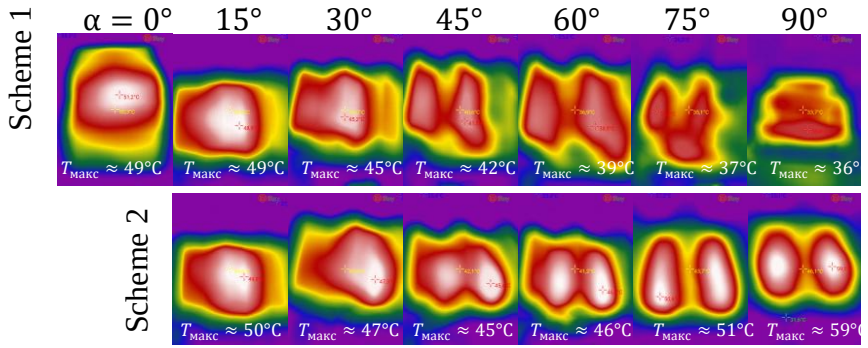

Fig. 2. Temperature field of the evaporation zone at different membrane inclination angles

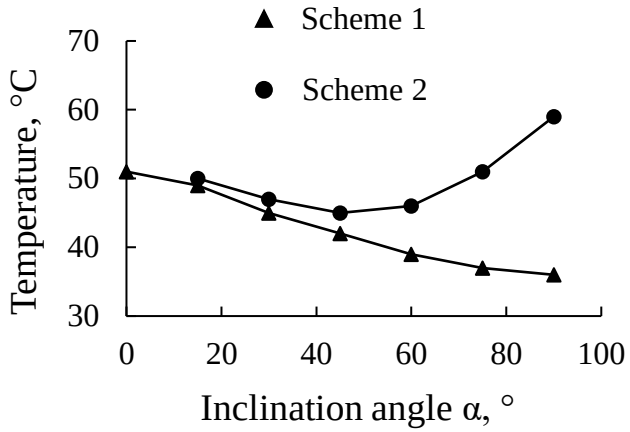

Fig. 3. Maximum evaporator surface temperatures

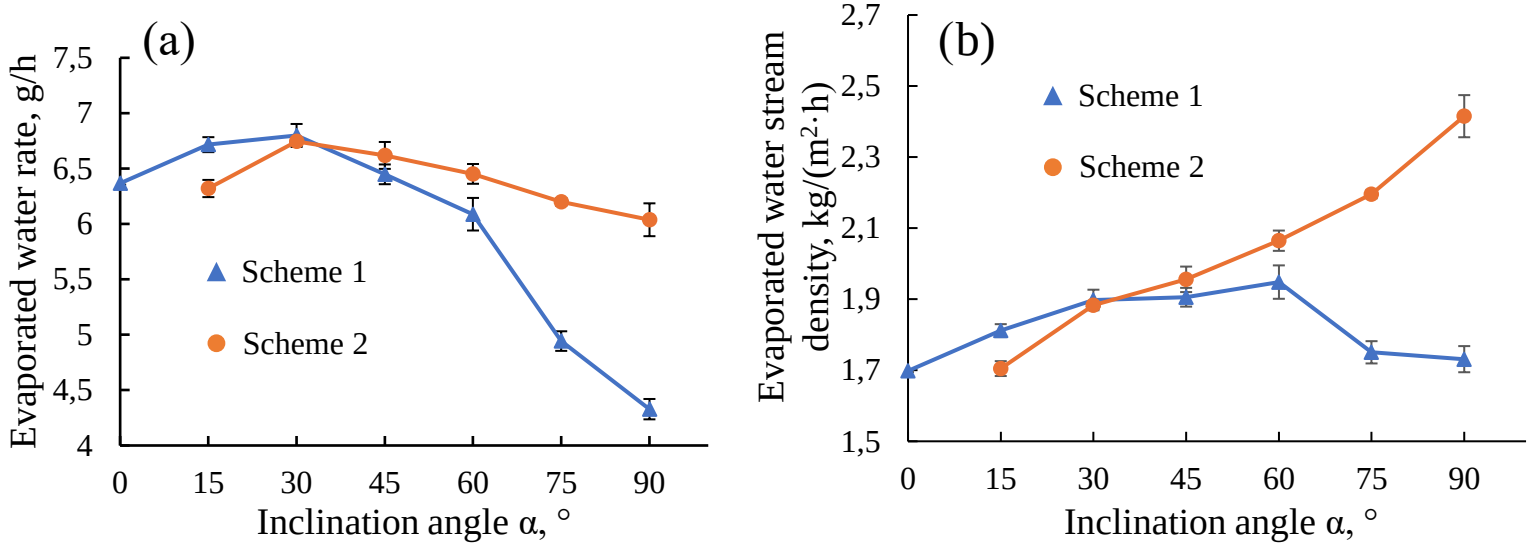

Fig. 4. Influence of the membrane angle on evaporator performance: flow rate (a) and density (b) of evaporated water.

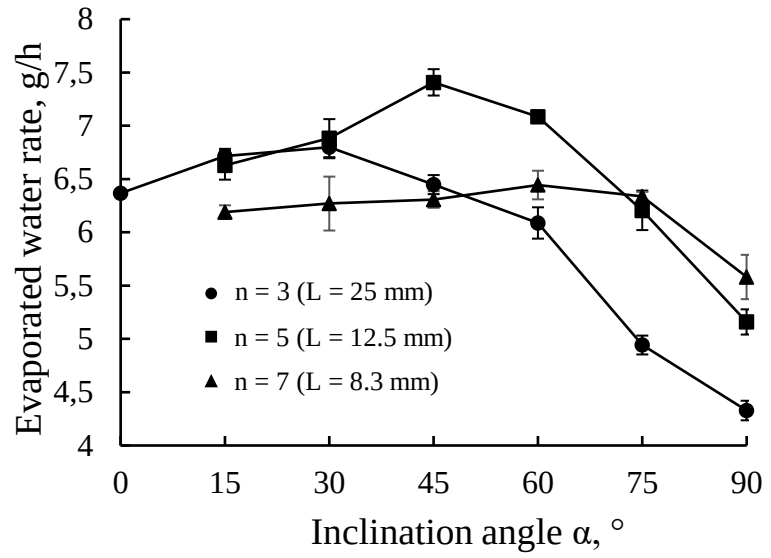

Fig. 5. Influence of the inclination angle and density of membranes in the evaporation zone on steam production productivity

Graphene hydrogel membranes for improving the efficiency and stability of solar evaporation

Desalination experiment with optimal evaporation zone configuration

Initial salt concentration = 3.5%

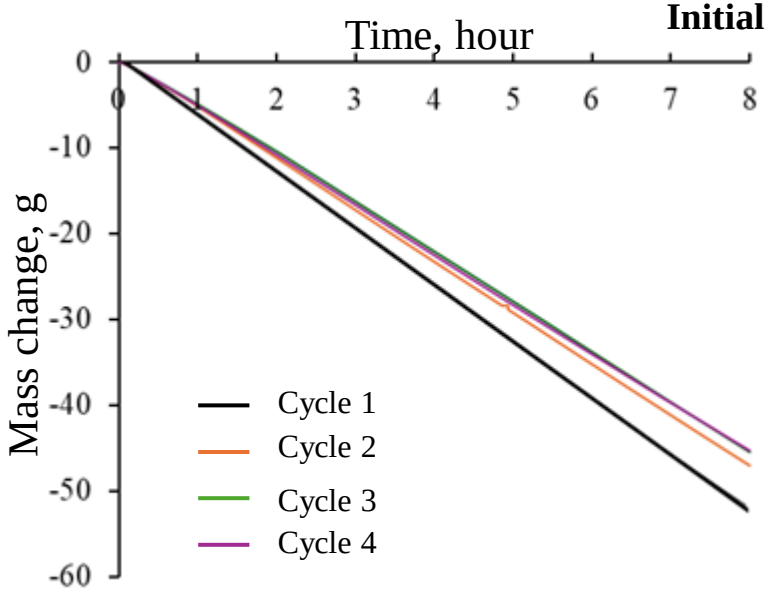

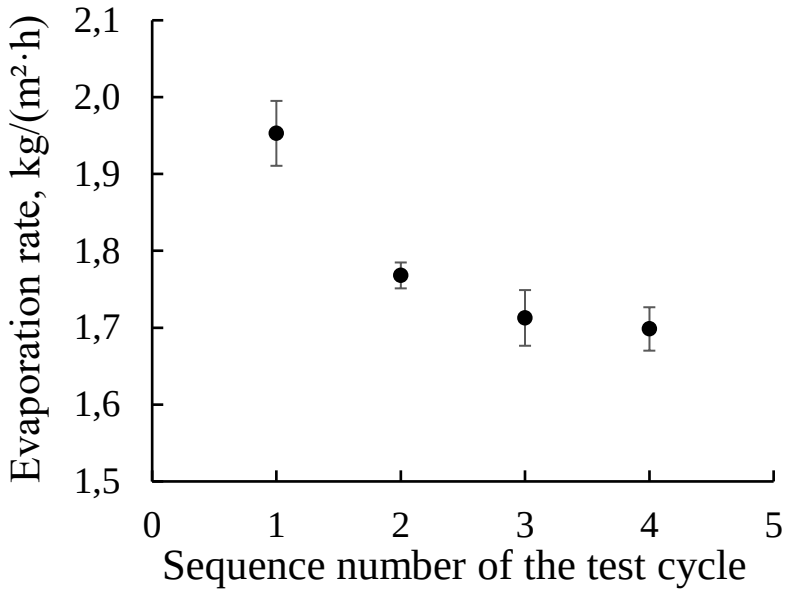

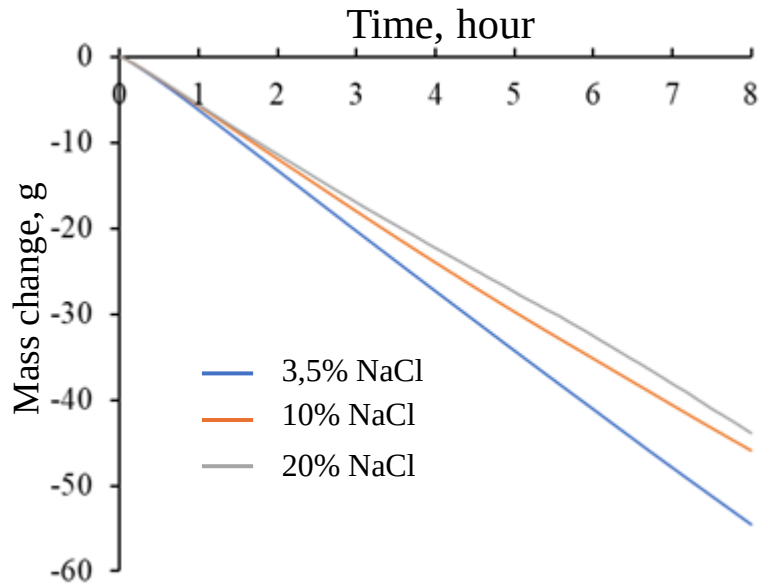

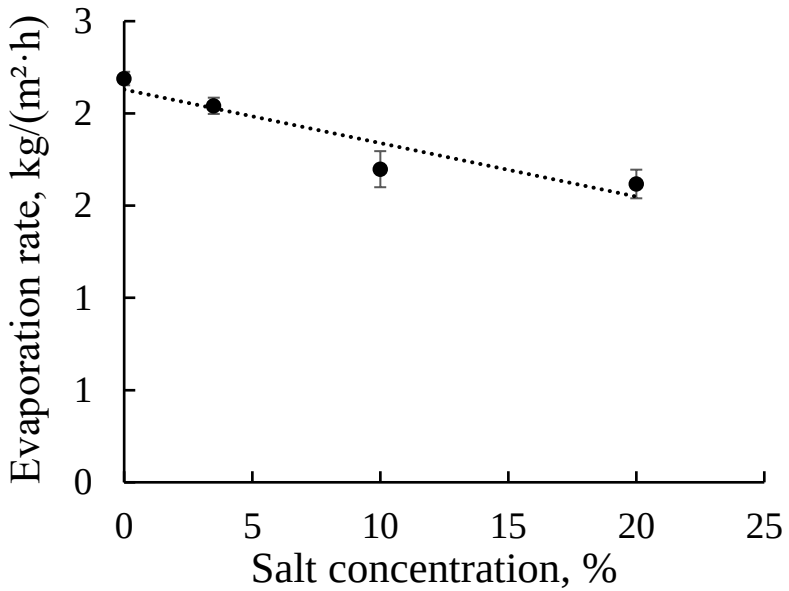

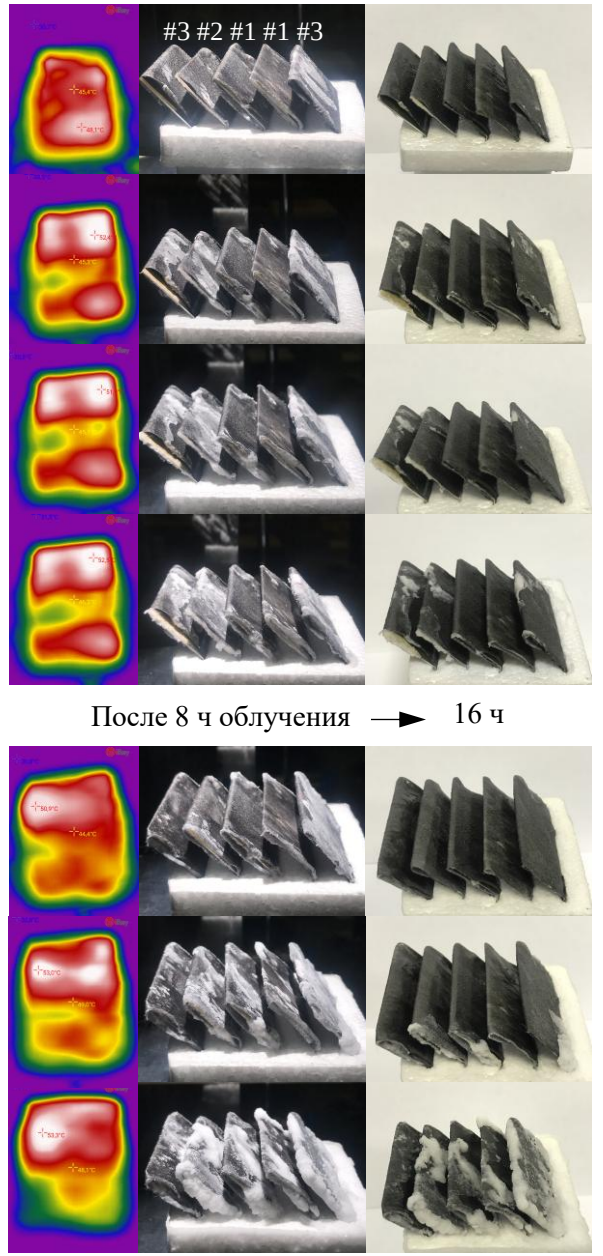

MODELING OF HEAT AND MASS TRANSFER PROCESSES IN A SOLAR EVAPORATOR

Evaporation model from the solar evaporator surface

Problem statement: development of a one-dimensional model of heat and mass transfer during evaporation from the solar evaporator surface.

Assumptions:

1. The evaporation zone is described as liquid water with an absorption coefficient of A = 1.
2. The thermophysical properties of water and moist air outside the interphase zone are constant.
3. The initial temperature is uniform and evenly distributed throughout the volume of the liquid layer.
4. Heat losses due to radiation are not taken into account.
5. Convection of the liquid in the liquid layer is ignored.
6. The mixture of dry air and water vapor is considered an ideal gas.

$$T_\infty = \text{const}; \rho_\infty = \text{const}; \varphi_\infty = \text{const}$$

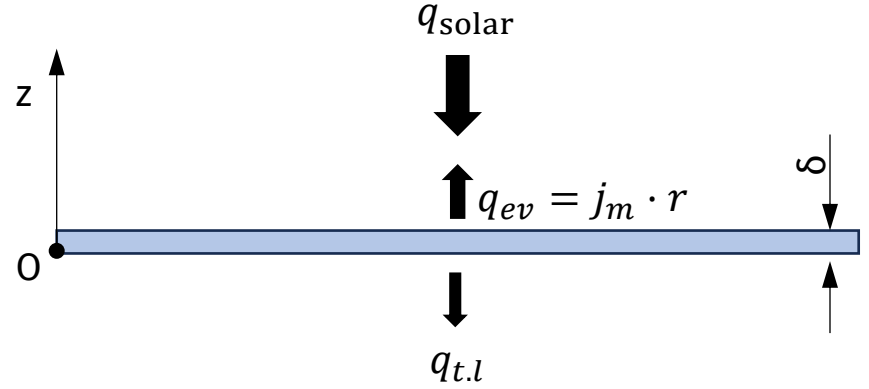

$$\rho \cdot c \cdot \frac{\partial T}{\partial t} = \lambda \cdot \frac{\partial^2 T}{\partial z^2}, \quad (1)$$

Initial and boundary conditions:

$$T(z, t = 0) = T_0, \quad (2)$$

$$-\lambda \frac{\partial T}{\partial z}\Big|_{z=\delta} = A \cdot q_{solar} - j_{evap} \cdot L_{eff}, \quad (3)$$

$$-\lambda \frac{\partial T}{\partial z}\Big|_{z=0} = q_{t.l}, \quad (4)$$

where δ = 0.2 mm is the thickness of the liquid layer; L_{eff} is the effective latent heat of evaporation; $q_{t.l}$ is the specific heat loss across the depth of the evaporator.

$$j_{evap} = \frac{Sh \cdot D}{L}[\rho_s(T_s) - \rho_s(T_\infty)]. \quad (5)$$

where $\text{Sh} = \text{B} \cdot \text{Ra}^{\text{m}}$ is the Sherwood number. For $2 \cdot 10^4 \le \text{Ra} \le 1.6 \cdot 10^6$: $\text{Sh} = 0.261 \cdot \text{Ra}^{307}$.

$$Ra = \frac{g \cdot (\rho_\infty - \rho_s) \cdot L^3}{\bar{\rho} \cdot \nu \cdot a}, \quad (6)$$

where g is the gravity acceleration; $(\rho_\infty - \rho_s)$ is the difference between the densities of the vapor-air mixture in the environment (ρ_∞) and on the water surface (ρ_s); $\bar{\rho}$ – average density of moist air; ν, a − kinematic viscosity and thermal conductivity coefficient of air, respectively.

$$\rho_s(T) = \frac{p_s(T)}{R_v T} = \frac{133 \cdot 10^{8.07131 - \frac{1730.63}{233.426+T}}}{R_v T}, \quad (7)$$

$$\rho_\infty(T) = \frac{28.96 p_{atm} - 10.94 \cdot \varphi \cdot p_s}{8314 T}. \quad (8)$$

MODELING OF HEAT AND MASS TRANSFER PROCESSES IN A SOLAR EVAPORATOR

Evaporation model from the solar evaporator surface

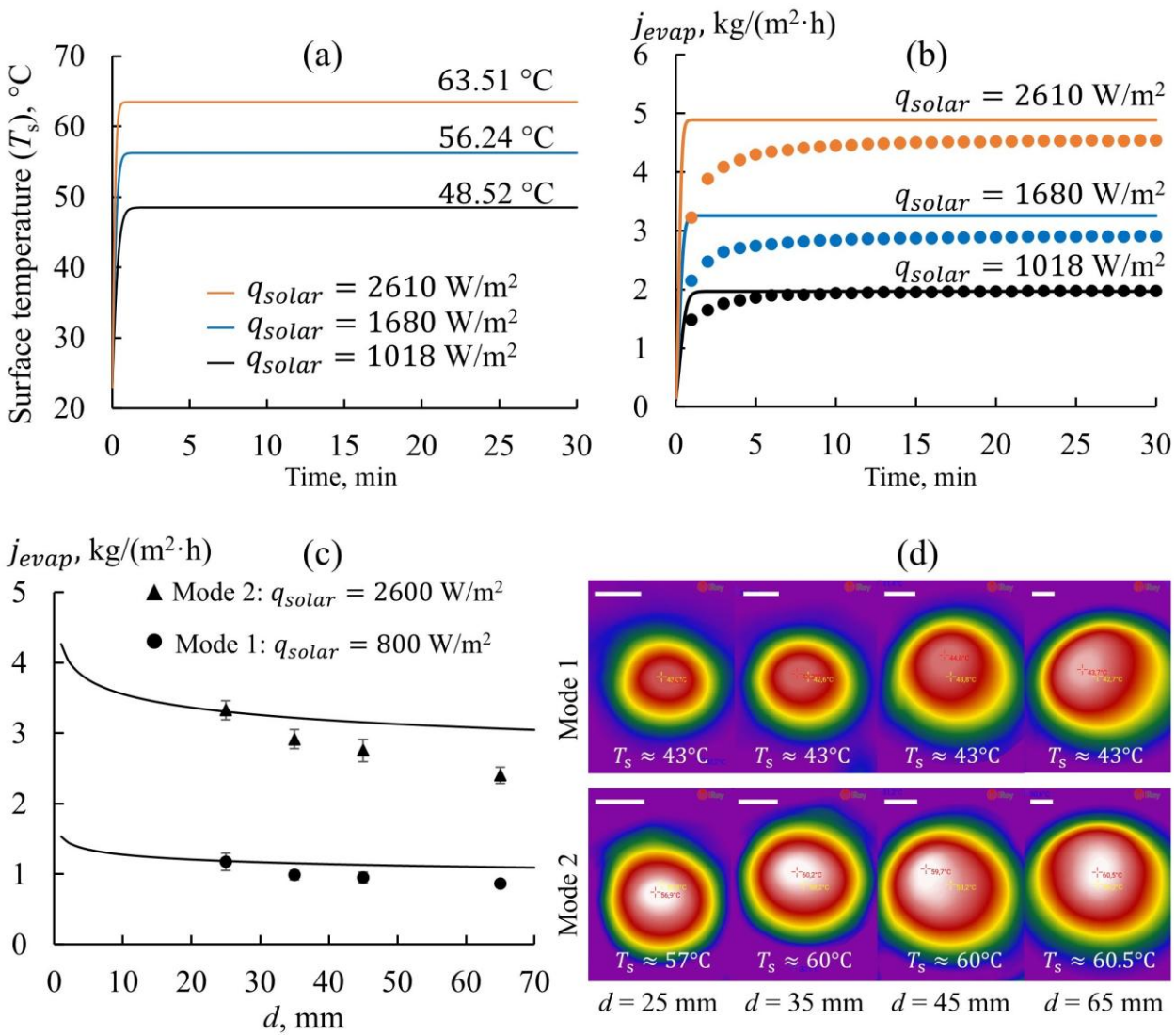

Fig. 1. Comparison of calculated (lines) and experimental (points) data for a 2D evaporator: characteristics of a sample with a diameter of 43 mm (a, b) and the effect of surface area on evaporation rate (c, d).

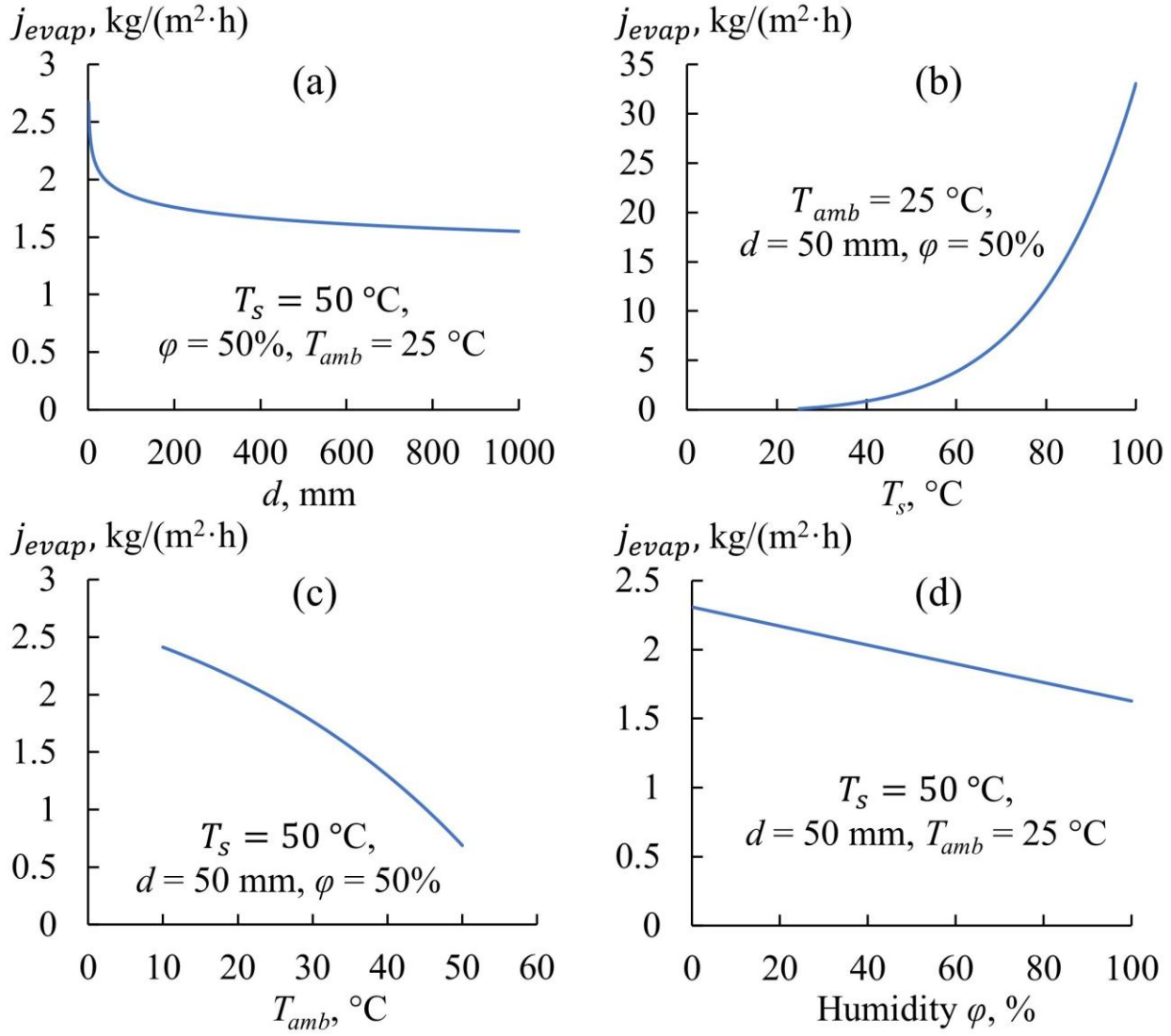

Fig. 2. Influence of evaporation area (a), environmental parameters (b, c), and surface temperature (d) on vaporization rate

KEY FINDINGS AND RESULTS OF THE STUDY

- A 2D prototype of a solar evaporator based on graphene-modified nonwoven material was created and studied for the first time; a method for evaluating its photothermal efficiency was proposed, and solar desalination tests were conducted.
- Graphene hydrogel membranes with a high vaporization rate of up to 2.4 kg/(m²·h), hydrophilicity, and self-cleaning from salt deposits were created for the first time; their geometry was optimized and their performance in salt water was confirmed.
- Mathematical model of heat and mass transfer in solar evaporators have been developed, describing the influence of external factors and the parameters of salt ion transfer.

THANK YOU FOR YOUR ATTENTION!